

## INTRODUCTION

Low emittance muon beams are central to the development of facilities such as a Neutrino Factory or a Muon Collider. The international Muon Ionization Cooling Experiment (MICE) was designed to demonstrate and study the cooling of muon beams. A study of the change in normalized transverse emittance in a flipped polarity magnetic field configuration is presented here.

## IONIZATION COOLING

The rate of change of normalized transverse emittance due to ionization cooling reads:

$$\frac{d\epsilon_{\perp}}{dz} \simeq -\frac{1}{\beta^2} \frac{\epsilon_{\perp}}{E_{\mu}} \left| \frac{dE_{\mu}}{dz} \right| + \frac{\beta_{\perp} (13.6 \text{ MeV})^2}{2\beta^3 E_{\mu} m_{\mu} c^2} \frac{1}{X_0}$$

Cooling is realised via the first term due to energy loss, while the second term represents heating due to Coulomb scattering. Heating is reduced by using a low Z material and minimizing  $\beta_{\perp} = (\langle x^2 \rangle + \langle y^2 \rangle) / \epsilon_{\perp}$ .

Figure 1: Schematic layout of the MICE cooling channel (A). Magnet coils are shown in red, the absorber in green and the various detectors are individually marked. The modelled on-axis magnetic field along the length of the cooling channel is shown in B (black line). Hall probe measurements are included as verification, and the field strength at the position of the hall probes is shown in green (160 mm off-axis). The magnetic field flips polarity at the absorber.

## COOLING APPARATUS

In the MICE experiment an upstream beamline is used to capture pions emitted from the titanium target and transport the produced muons into a cooling channel. The cooling channel (figure 1 A) consists of 12 individually powered solenoid magnets, symmetrically placed up- and downstream of an absorber chamber which could be configured depending on the beam momentum and required betatron function ( $\beta_{\perp}$ ).

Upstream and downstream Particle ID (PID) detectors are used to improve the reconstruction algorithms and reject pion and electron contamination within the beam, while the trackers measure the momentum and position of each muon before and after passing through the absorber. A range of absorbers were used during data taking including a 65 mm Lithium Hydride disk (LiH), a 22 l Liquid Hydrogen vessel (LH<sub>2</sub>) and an empty drift space (No absorber).

## RECONSTRUCTION

The muon beam emittance was calculated by constructing the covariance matrix,  $\sigma_{ab}$ , using the covariances,  $\Sigma$ , of the position and momentum components of the individual muon tracks:

$$\Sigma = \begin{pmatrix} \sigma_{xx} & \sigma_{xp_x} & \sigma_{xy} & \sigma_{xp_y} \\ \sigma_{p_x x} & \sigma_{p_x p_x} & \sigma_{p_x y} & \sigma_{p_x p_y} \\ \sigma_{yx} & \sigma_{yp_x} & \sigma_{yy} & \sigma_{yp_y} \\ \sigma_{p_y x} & \sigma_{p_y p_x} & \sigma_{p_y y} & \sigma_{p_y p_y} \end{pmatrix}$$

The 4-dimensional normalised transverse emittance,  $\epsilon_{\perp}$ , of the beam can then be calculated using the determinant of the covariance matrix and the muon mass,  $m_{\mu}$ :

$$\epsilon_{\perp} = \frac{1}{m_{\mu}} \sqrt[4]{|\Sigma|}$$

Events were selected with a Time-of-Flight consistent with a muon of momentum 140 +/- 5 MeV/c, that did not cross any hard apertures that could cause scraping. The reconstructed upstream tracks were required to have good chi-square per degree of freedom values and be fully contained within the tracking volume. If a corresponding downstream track was also found it was subjected to the same goodness of fit criteria. Only events with a valid track up- and downstream were included in the analysis.

## BEAM SAMPLING

A beam selection algorithm based on rejection sampling was employed to account for imperfections in beam optics matching at the entrance into the cooling channel. Figure 3 shows the improved optics of a sampled beam in comparison with its parent. The betatron function oscillations in the upstream tracker are significantly dampened, resulting in a reduced  $\beta_{\perp}$  at the absorber. This leads to a decrease in heating due to scattering, thus improving the cooling performance.

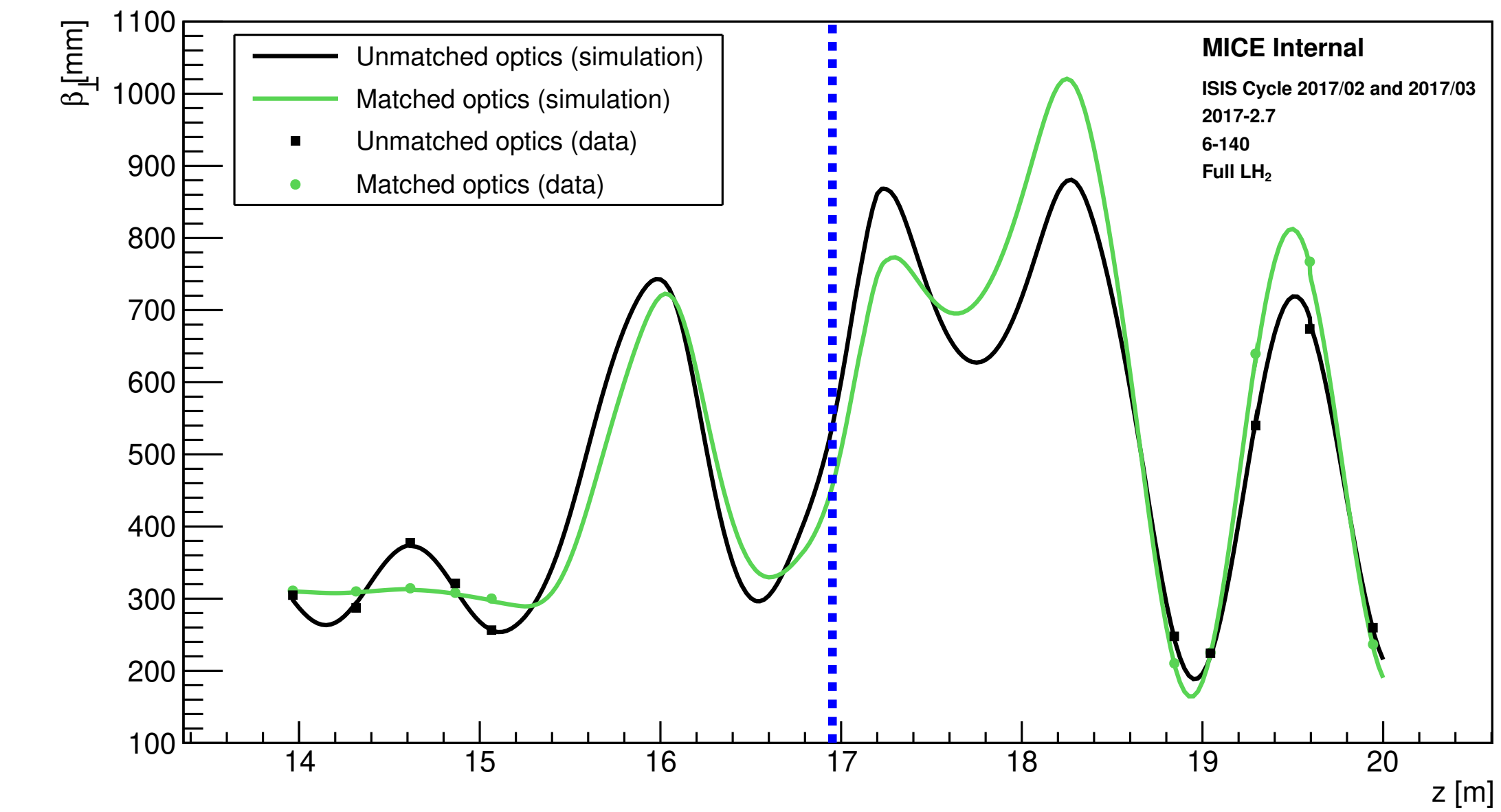


Figure 3: Comparison between the unmatched betatron function of the parent beam (black) and the improved optics of a beam sampled from the parent (green), using a rejection sampling algorithm tuned to match the beam optics in the upstream tracker. Good agreement between data (dots) and simulation (line) is observed at the tracker stations.

## EMITTANCE REDUCTION

The absolute change in emittance due to passage through the absorber module is shown in figure 4. The 'No absorber' case shows overall heating - emittance growth - due to optical aberrations induced by the large amplitude beam oscillations downstream of the absorber. In the case of the 'Empty LH<sub>2</sub>' vessel data, more heating is observed due to muon scattering in the aluminium windows. In both configurations, the emittance growth is independent of the input emittance.

The 'Full LH<sub>2</sub>' and 'LiH' cases demonstrate a clear emittance reduction for beams with initial emittance larger than ~2.7 mm and ~3 mm respectively. This is a signal of ionization cooling, a direct consequence of the presence of an absorber material in the cooling channel. At input emittance values below the equilibrium emittance, multiple Coulomb scattering dominates leading to heating. In both cases, the cooling effect increases linearly with initial emittance, as expected.

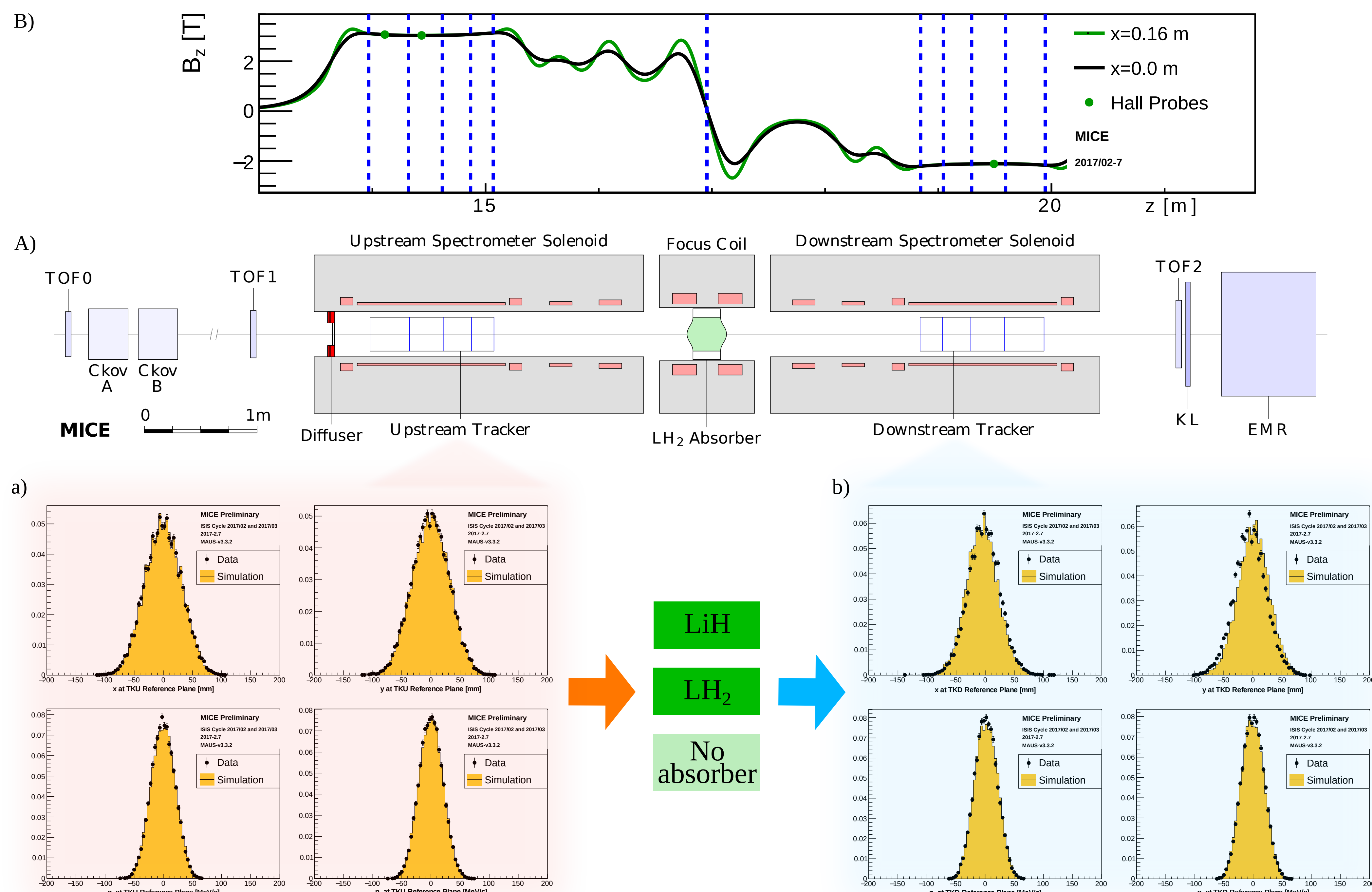


Figure 2: Distributions of the upstream (a) and downstream (b) position (top) and momentum (bottom) parameters in x (left) and y (right). All show good agreement between data and simulation. Measurement is performed at the tracker planes closest to the absorber module.

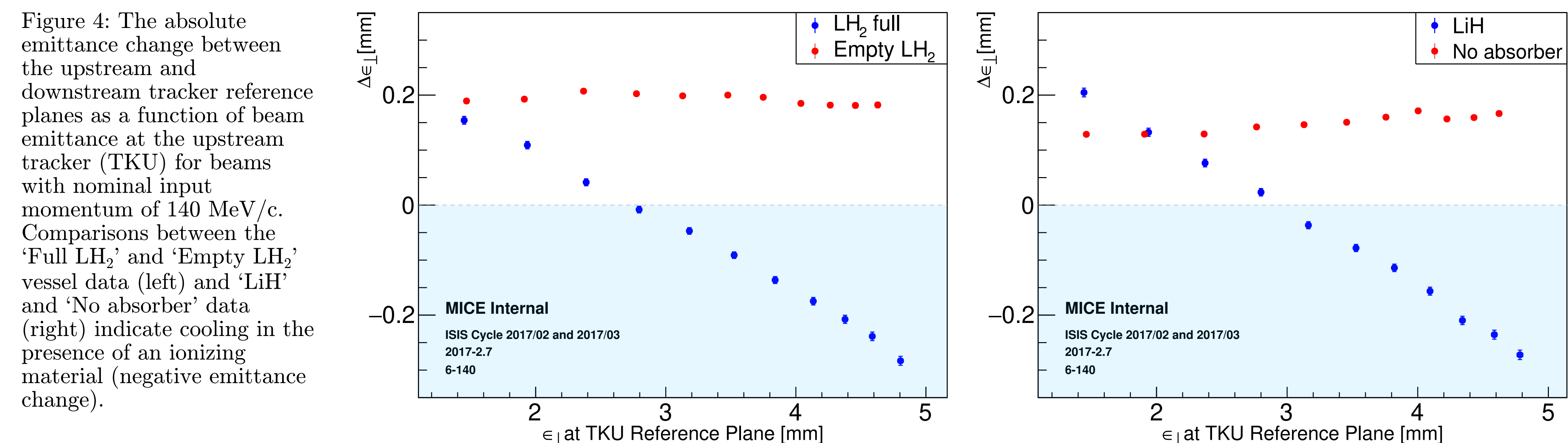


Figure 4: The absolute emittance change between the upstream and downstream tracker reference planes as a function of beam emittance at the upstream tracker (TKU) for beams with nominal input momentum of 140 MeV/c. Comparisons between the 'Full LH<sub>2</sub>' and 'Empty LH<sub>2</sub>' vessel data (left) and 'LiH' and 'No absorber' data (right) indicate cooling in the presence of an ionizing material (negative emittance change).

## ACKNOWLEDGEMENTS

The work described here was made possible by grants from Department of Energy and National Science Foundation (USA), the Instituto Nazionale di Fisica Nucleare (Italy), the Science and Technology Facilities Council (UK), the European Community under the European Commission Framework Programme 7 (AIDA project, grant agreement no. 262025, TIARA project, grant agreement no. 261905, and EuCARD), the Japan Society for the Promotion of Science and the Swiss National Science Foundation, in the framework of the SCOPES programme. We gratefully acknowledge all sources of support. We are grateful to the support given to us by the staff of the STFC Rutherford Appleton and Daresbury Laboratories and the Cockcroft Institute. We acknowledge the use of Grid computing resources deployed and operated by GridPP in the UK, <http://www.gridpp.ac.uk/>.